Bull. Chem. Soc. Jpn., ***69***, *71—76 (1996)*

Near-Threshold Photodissociation of C_2H_2, C_2HD, and C_2D_2 Studied by H(D) Atom Photofragment Translational Spectroscopy

Steven H. S. Wilson, Claire L. Reed, David H. Mordaunt,# Michael N. R. Ashfold, and Masahiro Kawasaki*,†

School of Chemistry, University of Bristol, Bristol BS8 1TS, U.K.

†Institute for Electronic Science and Graduate School of Environmental Science, Hokkaido University, Sapporo 060

(Received July 19, 1995)

The photodissociation of jet-cooled C_2H_2, C_2HD, and C_2D_2 molecules following excitation within their respective predissociated $\tilde{A}$-$\tilde{X}$ absorption band systems has been investigated using the technique of H(D) Rydberg-atom photofragment translational spectroscopy. Analyses of the rotational structure apparent in the resulting total kinetic-energy release spectra yields precise values for the DCC–H, HCC–D, and DCC–D bond dissociation energies: D_0^0(DCC–H) = 46144±50 cm^{-1}, D_0^0(HCC–D) = 46687±50 cm^{-1}, and D_0^0(DCC–D) = 46754±50 cm^{-1}, respectively. The average internal excitation of bending vibration in the C_2H(C_2D) fragments formed from these photolyses of all three parent isotopomers is shown to scale linearly with the excess energy over and above that required for bond fission by ca. 540 cm^{-1}.

Acetylene photolysis, and subsequent chemistry involving the ethynyl (C_2H) radical, both play important roles in establishing the hydrocarbon balance in the atmospheres of the outer planets and their moons.[1,2] Acetylene has a linear, $\tilde{X}^1\Sigma_g^+$, ground electronic state; its lowest lying excited electronic states result from a $\pi_g^*\leftarrow\pi_u$ promotion; the resulting excited states have planar, *trans*-bent equilibrium geometries. The $\tilde{A}^1A_u$–$\tilde{X}^1\Sigma_g^+$ ultraviolet absorption system of acetylene exhibits a wealth of resolved rovibronic structure in the 190—240 nm wavelength range; not surprisingly, these band systems in all three isotopomers (C_2H_2, C_2HD, and C_2D_2) have attracted much attention from spectroscopists.[3—15]

Although the $\tilde{A}$ state of acetylene correlates adiabatically with the products H+$C_2H(\tilde{A}^2\Pi)$, measurements of the parent $C_2H_2(\tilde{A}$–$\tilde{X})$ laser-induced fluorescence (LIF) excitation spectrum show a clear "breaking-off" at excitation wavelengths shorter than 216 nm, i.e. at energies well below the energetic threshold for forming such electronically excited fragments.[12,13] The nature of the competing excited state decay processes has been a subject of long-standing interest. Predissociation to ground-state products H+$C_2H(\tilde{X}^2\Sigma^+)$ is one obvious possibility. This could involve intersystem crossing to near the resonant levels of the first triplet (T_1) state, and/or internal conversion to very high vibrational levels of the ground state. The concensus view emerging from several recent high-resolution LIF studies[16,17] from quantum beat measurements[18,19] and from external magnetic effect on fluorescence[20] is that intersystem crossing represents the dominant nonadiabatic coupling mechanism in the energy range studied to date. There now exists a reasonable body of evidence that the quantum yield for the simple C–H bond fission channel, even at the wavelengths as short as 193.3 nm, is only 0.2—0.3.[21—23] Metastable triplet-state acetylene molecules[24] and, more recently, vinylidene (H_2CC) radicals in their $^3B_2$ state[25—28] have been proposed as sinks for that fraction of the photoprepared $C_2H_2(\tilde{A})$ molecules which apparently do not fragment. Clearly, a complete description of the photophysics of the $\tilde{A}$ state acetylene molecules remains a considerable challenging one that is now starting to be addressed by H(D) atom photofragment translational spectroscopy.[29]

The first photofragment translational spectroscopy study of C_2H_2 photolysis in this wavelength region, at 193.3 nm, was reported by Wodtke and Lee.[30] These workers monitored the C_2H fragments, which they deduced to be formed both in the ground, $\tilde{X}$, and first excited, $\tilde{A}$, electronic states. They also saw clear evidence of facile secondary photolysis of the nascent C_2H products (yielding C_2 radicals and another H atom), and deduced a value for the primary bond dissociation energy of D_0(H–CCH) = 46200±700 cm^{-1}, in good accord with contemporary values determined by other experiments[31,32] and by theory.[33] Two groups[34,35] subsequently reported significantly lower values for this bond strength, which, in turn, triggered a flurry of both theoretical[36—38] and experimental[39—42] activity. These more recent studies all pointed to the general correctness of the Wodtke and Lee value, a conclusion that was vindicated by our recent preliminary high-resolution H-atom photofragment translational spectroscopy study of C_2H_2 photolysis.[43] Here, we report on the results of similar high-resolution studies of the C–H and C–D fission channels in C_2HD and C_2D_2, at a range of near-UV excitation wavelengths, and provide some of the first quantitative data on energy disposal in the

---

#Present address: Max-Planck-Institut für Strömungforschung, 37073 Göttingen, Germany.

resulting $C_2H(C_2D)$ photofragments.

Experimental

The photofragment translational spectrometer and laser systems used in this study have been fully described elsewhere.[44] In brief, a skimmed pulsed supersonic beam of acetylene (typically 5% HCCH or HCCD or DCCD seeded in 95% Ar, at a total stagnation pressure of ca. 1 bar) is crossed at right angles by the output of various pulsed laser systems used to effect the photolysis and to 'tag' the nascent hydrogen atoms. The photolysis laser UV radiation was tuned to absorption resonances located by a complementary resonance-enhanced multiphoton ionisation (REMPI) study of acetylene.[15] The recoil kinetic-energy distribution of these tagged H(D) atoms is determined by measuring their collision-free times-of-flight to a detector (a Johnston multiplier, type MM1-SG) positioned along the third orthogonal axis with its front face either 825 mm distant from the interaction region in the studies of HCCH photolysis or 425 mm in the case of the HCCD and DCCD studies. Increasing the flight path improves the kinetic-energy resolution of the resulting total kinetic-energy release (TKER) spectrum, by decreasing the solid angle subtended at the detector from the interaction region. However, the use of a longer flight tube was only possible for the photolysis of HCCH, where signal strengths were sufficiently high to cope with the concomitant loss of signal associated with the smaller detector acceptance angle.

The UV photolysis studies of acetylene presented here require three laser systems. The photolysis laser system consists of a Nd–YAG pumped dye laser system (Quanta-Ray GCR-5, PDL-3) operating on DCM dye, producing light in the 660—615 nm wavelength region. This radiation was frequency tripled, i.e. the fundamental dye-laser radiation was frequency doubled in a KDP crystal; then, the doubled and fundamental dye laser radiation were mixed in a BBO crystal, yielding tunable coherent light in the 220—205 nm range. A home-built Soleil–Babinet compensator was employed to reorient the polarisations of the doubled and fundamental beams, before entering the BBO crystal, in order to optimise the mixing process. The light was then focused with a lens (f=500 mm) so as to overlap spatially, and immediately precede within 5 ns, the hydrogen-atom tagging pulses described below, in the interaction region.

Tagging of the H(D) atoms is achieved at the source using two additional laser systems. One provides radiation at the $H_{Ly-\alpha}$ and $D_{Ly-\alpha}$ wavelengths, 82259 and 82280 cm^{-1}, respectively, to excite at the line centre of the $n=2 \leftarrow n=1$ transition of the nascent H(D) atoms. The second laser system operates at wavelengths ca. 365 nm, to further promote the H(D) atoms in n=2 to high Rydberg states ($n \approx 70$) lying just below the ionization threshold. As before,[43] the necessary vacuum ultraviolet (VUV) radiation was generated by frequency tripling, in krypton, 364.6 nm (364.5 nm for D atoms) light, which in turn was produced by sum-frequency mixing the 1064 nm fundamental output of a Nd–YAG pump laser (Continuum YG 682-10) with dye laser radiation at ca. 554.7 nm (554.5 nm). The 365 nm light used in the second step of the double-resonant excitation of the H(D) atoms was produced by frequency doubling in a DCDA crystal the output of a second dye laser (Spectron SL4000G) pumped by the same Continuum Nd–YAG laser.

The various ultraviolet and vacuum ultraviolet beams were focused into the interaction region, with a crossing angle of ca. 6°, so as to overlap in time and space. Rydberg atoms excited in this way fly from the interaction volume; those that happen to recoil along the time-of-flight (TOF) axis are field ionized immediately prior to striking the Johnston multiplier. A pair of suitably biased annular electrodes that provided a field strength of ca. 2 $V\,mm^{-1}$, positioned at either side of the interaction volume, ensured that any ions formed by the initial laser excitations were extracted at the source, and, thus, did not contribute to the measured TOF spectrum. Checks were made to ensure that all of the observed signal depended on the presence of all three laser beams, i.e. to ensure that neither probe beam caused any detectable photolysis.

The output from the multiplier was amplified and sent to a digital storage oscilloscope (LeCroy 9450, 350 MHz bandwidth) for visual display. The signal was also transferred on a shot-by-shot basis, via a parallel interface, to an IBM PS/2 for accumulation and subsequent data processing.

DCCD was prepared by reacting D_2O with calcium carbide on a glass vacuum line, that had been previously exposed to D_2O, in order to deuterate the glass surfaces of the vacuum line. HCCD was prepared by a similar method, but a 50 : 50 mixture of D_2O and H_2O was used. No attempt was made to purify the resulting mixture of HCCD, DCCD, and HCCH since the jet-cooled UV absorption spectra of the three isotopomers are sufficiently sparse and structured[15] that it is possible to excite selectively the HCCD isotopomer. HCCH and the argon carrier gas were obtained commercially and used as supplied.

Results and Discussion

1. Bond Dissociation Energies.

Figure 1 shows a TOF spectrum of H Rydberg atoms resulting from the photolysis of jet-cooled HCCD at 210.868 nm. This photolysis wavelength, using the assignments and nomenclature of reference,[15] excites the overlapping, predissociated $\tilde{A}$–$\tilde{X}$ $V^3_0 6^4_0 K^1_0$ and $2^1_0 V^4_0 K^1_0$ transitions of HCCD. An analysis of this and the other TOF spectra recorded in this study was carried out, following past procedures,[44] by transforming the TOF data into a spectrum of total kinetic-energy release (*TKER*) of the fragment as shown in Fig. 2, using the relationship

$$TKER = \frac{1}{2} m_H \left(1 + \frac{m_H}{m_{DCC}}\right) \left(\frac{d}{t_H}\right)^2, \tag{1}$$

which assumes conservation of the total energy and linear momentum. In this equation, t_H is the measured H-atom TOF, and d is the flight distance. Considering energy conservation

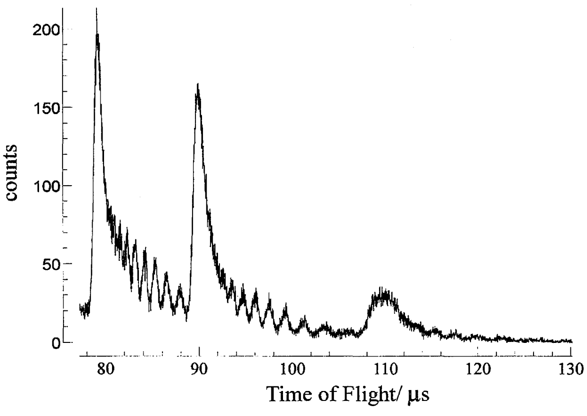

Fig. 1. TOF spectrum of H atms resulting from the linearly polarised (ε_{phot} perpendicular to the TOF axis) photolysis of a jet-cooled sample of HCCD at 210.868 nm. This photolysis wavelength excites the overlapping, predissociated $\tilde{A} \leftarrow \tilde{X}$ $V^3_0 6^4_0 K^1_0$ and $2^1_0 V^4_0 K^1_0$ transitions of HCCD.[15]

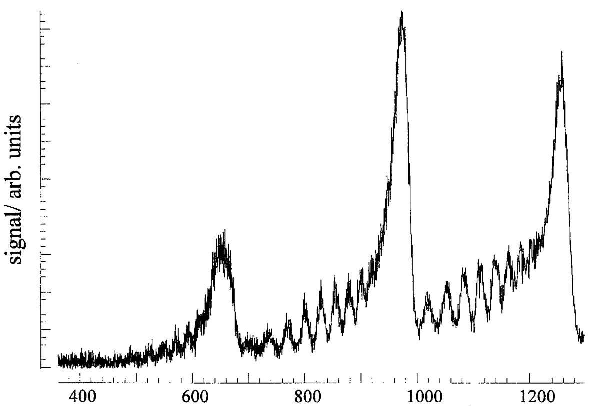

Fig. 2. Total kinetic energy release (TKER) spectrum of the H+CCD fragments resulting from photolysis of jet-cooled HCCD at 210.868 nm.

for photolysis,

$$h\nu + E_{\mathrm{parent}} = D_0^0(\mathrm{DCC{-}H}) + E_{\mathrm{DCC}} + TKER, \qquad (2)$$

where $h\nu$ is the photolysis energy and E_{DCC} is the internal excitation of the DCC fragment. E_{parent}, the parent internal state, is well-defined, since the jet-cooled absorption spectrum is sufficiently structured that the photolysis energy defines a very narrow subset of rovibronic transitions.

Clearly, in order to determine the internal energy distribution of the DCC fragment we require the bond dissociation energy, D_0^0(DCC–H). At threshold, i.e. when $E_{\mathrm{int,DCC}}=0$

$$D_0^0(\mathrm{DCC{-}H}) = h\nu + E_{\mathrm{parent}} - TKER. \qquad (3)$$

Thus, given that E_{parent} is small and that the photon energy is well-defined, establishing the bond strength simply requires an accurate determination of the maximum *TKER* that corresponds to the formation of DCC($\tilde{X}\,^2\Sigma^+$, v=0, N=0) fragments. As in previous studies,[43] we determined this threshold by fitting the observed spectrum to the known DCC rotational eigenvalues[45] (Fig. 3). The combs superimposed on Fig. 3 confirm that this is the case. Similar analyses of the TOF spectra of D atoms resulting from the 205.950 nm photolysis of HCCD and from the 209.266 nm photolysis of DCCD (Fig. 4) yielded values of D_0^0(HCC–D)=46687±50 cm^{-1} and D_0^0(DCC–D)=46754±50 cm^{-1}, respectively.

We now proceed to demonstrate that these values are wholly consistent with the earlier determination[43] of D_0^0(HCC–H)=46074±8 cm^{-1}. Tables 1 and 2 list the harmonic vibrational wavenumbers for the various normal vibrational modes of the parent isotopomers (HCCH, HCCD, and DCCD) and of the fragments (HCC, DCC), respectively. D_e(H–CCH), which in the Born–Oppenheimer limit, should be independent of the isotope substitution, and is given by

$$D_e(\mathrm{HCC{-}H}) = D_0^0(\mathrm{HCC{-}H}) + \varepsilon_0(\mathrm{HCCH}) - \varepsilon_0(\mathrm{HCC}), \qquad (4)$$

where ε_0 is the zero-point energy of the particular species. Given the vibrational wavenumbers listed in Tables 1 and 2, we obtained the zero-point energies for the various parent molecules and fragments shown in these tables. Given ε_0(HCCH) and ε_0(HCC), we thus obtained a value D_e(HCC–H)=48795 cm^{-1}. This D_e value, together with the other ε_0's, allows a calculation of D_0^0(DCC–H), D_0^0(HCC–D), and D_0^0(DCC–D). These calculated values are in excellent agreement those determined in the present study (Table 3).

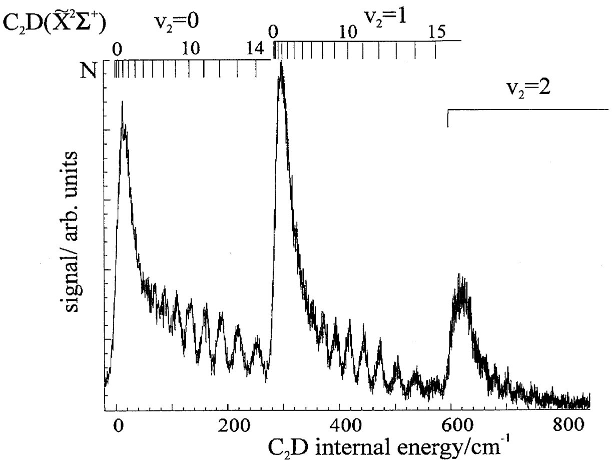

Fig. 3. Internal energy spectrum of the C$_2$D fragments derived from the total kinetic energy spectrum shown in Fig. 2 (210.868 nm photolysis of HCCD). Combs superimposed above the spectrum indicate the energies of various rotational states of the C$_2$D($\tilde{X}$) fragment in both its ground (v_2=0) and first excited bending (v_2=1) levels. In constructing the latter comb we assume the rotational constants for the v_2=1 level to be the same as those for the zero-point level.

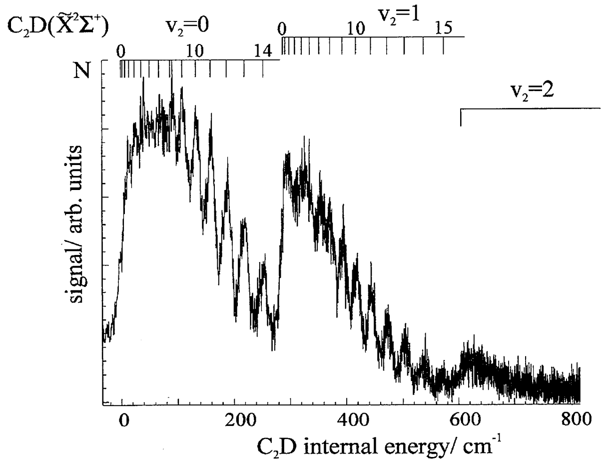

Fig. 4. Internal energy spectrum of the C$_2$D fragments derived from a D atom TOF spectrum resulting from the linearly polarised ($\varepsilon_{\mathrm{phot}}$ perpendicular to the TOF axis) photolysis of a jet-cooled sample of DCCD at 209.266 nm. This photolysis wavelength excites the predissociated $\tilde{A}\leftarrow\tilde{X}$ $1_0^1V_0^4K_0^1$ transition of DCCD. Combs superimposed above the spectrum indicate the energies of various rotational states of the C$_2$D($\tilde{X}$) fragment in both its ground (v_2=0) and first excited bending (v_2=1) levels.

2. Dissociation Dynamics. TOF spectra of the H(D) atoms have been recorded at a series of different excitation

Table 1. Harmonic Vibrational Frequencies[a)] and Zero Point Energies (ε_0) for HCCH, HCCD, and DCCD

	HCCH	HCCD	DCCD
	cm^{-1}	cm^{-1}	cm^{-1}
ω_1	3373	3335	2701
ω_2	1974	1851	1762
ω_3	3295	2584	2427
ω_4	612	519	509[b)]
ω_5	729	683	538[b)]
ε_0	5662	5087	4492

a) Ref. 45. b) Ref. 46.

Table 2. Harmonic Vibrational Frequencies[a)] and Zero Point Energies (ε_0) for HCC and DCC

	HCC	DCC
	cm^{-1}	cm^{-1}
ω_1	3298.85[b)]	2537.1[b)]
ω_2	371.60	285[c)]
ω_3	1840.57	1743.18
ε_0	2941	2425

a) Ref. 47. b) Ref. 48. c) Value obtained from data presented in Fig. 3, in good agreement with estimate presented in Ref. 48.

Table 3. Comparison of Calculated with Experimental Bond Dissociation Energies for the Various Isotopomers of Acetylene

	D_0^0(Calcd)	D_0^0(Experimental)
	cm^{-1}	cm^{-1}
DCC–H	46133	46144±50
HCC–D	46649	46687±50
DCC–D	46728	46754±50

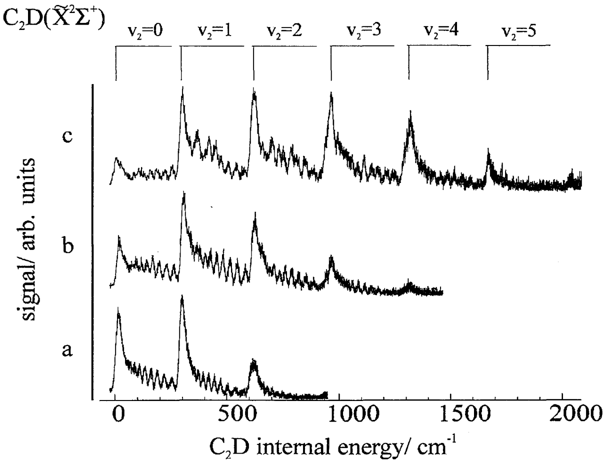

Fig. 5. Internal energy spectra of the C_2D fragments derived from H atom TOF spectra resulting from the linearly polarised ($\varepsilon_{\mathrm{phot}}$ perpendicular to TOF axis) photolysis of HCCD at (a) 210.868 nm, (b) 208.602 nm, and (c) 205.950 nm. These photolysis wavelengths excite the predissociated $\tilde{A}\leftarrow\tilde{X}$ $V_0^3 6_0^4 K_0^1$ and $2_0^1 V_0^4 K_0^1$ (overlapping), $V_0^3 6_0^5 K_0^1$ and $2_0^2 6_0^6 K_0^1$ transitions of HCCD, respectively.[15)] Combs superimposed above the spectra indicate a progression in the ν_2 (bending) mode of $C_2D(\tilde{X})$.

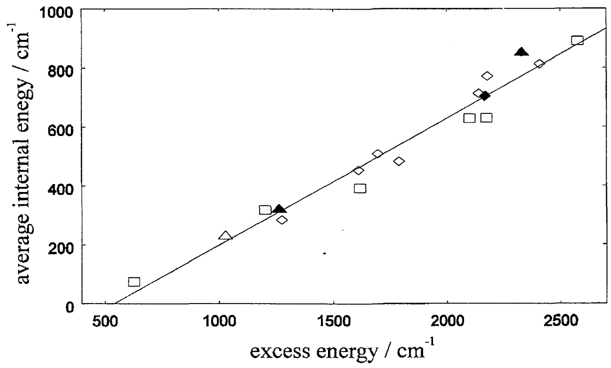

Fig. 6. Plot of average fragment internal excitation as a function of excess energy for the photolyses HCC–H (□), DCC–D (△), and DCC–H (◇). Filled symbols indicate that the excitation originated from vibrationally excited parent molecules with $v_4''=1$. The solid line indicates the best-fit between all the points.

wavelengths for each of the acetylene isotopomers. Figure 5 shows three DCC internal energy spectra derived from the H-atom TOF spectra resulting from the photolysis of HCCD at 210.868, 208.602, and 205.933 nm. These photolysis wavelengths correspond to, respectively, the overlapping $V_0^3 6_0^4 K_0^1$ and $2_0^1 V_0^4 K_0^1$ transitions, the $V_0^3 6_0^5 K_0^1$ band and the $2_0^2 6_0^6 K_0^1$ band of the predissociated $\tilde{A}\leftarrow\tilde{X}$ system of HCCD.[15)] The spectra show an increase in the DCC internal excitation as the photolysis energy increases. The ν_2 bending-vibrational mode in the DCC fragment appears to be particularly active, as might be expected on Franck–Condon grounds, given the planar *trans*-bent ← linear change in equilibrium geometry of acetylene that accompanies the parent $\tilde{A}\,^1A_u\leftarrow\tilde{X}\,^1\Sigma_g^+$ transition. Similar trends are observed in the spectra resulting from the photolysis of HCCH and from DCCD. In an attempt to quantify this trend, we calculated the average internal excitation (E_{int}), as a function of the excess energy, $E_{\mathrm{excess}}=h\nu-D_0^0$. Figure 6 shows a plot of the deduced E_{int} of the fragment versus E_{excess} for the photolysis of all three isotopomers. This correlation is linear and is coincidental for all three species. The extent of fragment internal excitation appears to be insensitive to the particular parent vibronic excitation; also, we do not see any marked isotope effect in the energy disposal. The gradient of the best-fit line through all of the points provides the ratio $E_{\mathrm{int}}/E_{\mathrm{excess}}=0.43$, while the plot intercepts the excess energy axis at a value of 540 cm^{-1}.

As mentioned in Introduction, there now exists a large body of evidence[12,13,16—23)] pointing to the influence of singlet–triplet interactions on the $\tilde{A}\,^1A_u$ state of acetylene at energies somewhat lower than those relevant in the present study. Pivotal amongst these are the studies of Ochi and Tsuchiya,[19)] who showed the effect of a magnetic field on the decay profiles of the parent $\tilde{A}\rightarrow\tilde{X}$ emission, and the high-resolution laser-induced fluorescence spectra of Drabbels et al.,[17)] which imply a density of "background" states coupled to any particular rovibronic level of the $\tilde{\mathrm{A}}\,^1\mathrm{A}_\mathrm{u}$ state that is fully compatible with an assumed S_1–T_1 coupling. Additionally, there now appears to be a reasonable concensus that the low primary fragment quamtum yield reported at shorter wavelengths, including 193.3 nm ($\Phi\approx0.2$—0.3),[23] can be attributable to alternative non-dissociative processes, e.g. intersystem crossing and isomerisation to the vinylidene structure on a triplet potential energy surface.[20—28] The present observations also appear to be wholly consistent with a model in which the $\tilde{\mathrm{A}}\,^1\mathrm{A}_\mathrm{u}$ state acetylene molecules predissociate via intersystem crossing to near-resonant levels of the T_1 triplet excited state, whose subsequent fragmentation to ground state products involves passage through a rather tightly constrained transition state, the saddle points, for which lies some 540 cm^{-1} above the asymptotic energy associated with ground state fragment products. A full discussion of the dynamical implications of these findings, of the detailed rovibronic energy disposal in the resulting HCC and DCC fragments, and of the angular anisotropy of the recoiling H fragments, is reserved for a future publication.

The Bristol group wishes to acknowledge the long-standing help, advice and encouragement given by Professor K. H. Welge and Dr. L. Schnieder of Universität Bielefeld and by Professor R. N. Dixon and K. N. Rosser of University of Bristol, as well as the financial support of this work from EPSRC and NERC. MNRA and MK are grateful to the Royal Society for the award of a Leverhulme Trust Senior Research Fellowship and the Japan Society for Promotion of Science for a Japan–UK Cooperative Program, respectively. DHM is grateful to the European Community for the award of an individual research fellowship under the Human Capital and Mobility Program, and SHSW thanks the B'nai Brith Scholarship Committee for additional financial support.

References

1) M. Allen, Y. L. Yung, and G. R. Gladstone, *Icarus*, **100**, 527 (1992).

2) R. P. Wayne, *J. Geophys. Res.*, **98**, 13119 (1993).

3) C. K. Ingold and G. W. King, *J. Chem. Soc.*, **1953**, 2702.

4) K. K. Innes, *J. Chem. Phys.*, **22**, 863 (1954).

5) J. K. G. Watson, M. Herman, J. C. Van Craen, and R. Colin, *J. Mol. Spectrosc.*, **95**, 101 (1982).

6) J. C. Van Craen, M. Herman, R. Colin, and J. K. G. Watson, *J. Mol. Spectrosc.*, **111**, 185 (1985).

7) J. C. Van Craen, M. Herman, R. Colin, and J. K. G. Watson, *J. Mol. Spectrosc.*, **119**, 137 (1986).

8) T. R. Huet and M. Herman, *J. Mol. Spectrosc.*, **132**, 361 (1988).

9) J. Vander Auwera, T. R. Huet, M. Herman, C. Hamilton, J. L. Kinsey, and R. W. Field, *J. Mol. Spectrosc.*, **137**, 381 (1989).

10) T. R. Huet and M. Herman, *J. Mol. Spectrosc.*, **137**, 396 (1989).

11) C. Hamilton, R. W. Field, T. R. Huet, and M. Herman, *J. Mol. Spectrosc.*, **137**, 427 (1989).

12) M. Fujii, A. Haijima, and M. Ito, *Chem. Phys. Lett.*, **150**, 380 (1988).

13) A. Haijima, M. Fujii, and M. Ito, *J. Chem. Phys.*, **92**, 959 (1990).

14) J. D. Tobiason, A. L. Utz, E. L. Sibert, III, and F. F. Crim, *J. Chem. Phys.*, **99**, 5762 (1993).

15) A. J. Orr-Ewing, R. A. Morgan, S. H. S. Wilson, C. L. Reed, and M. N. R. Ashfold, *J. Chem. Soc., Faraday Trans.*, in press.

16) G. J. Scherer, Y. Q. Chen, R. L. Redington, J. L. Kinsey, and R. W. Field, *J. Chem. Phys.*, **85**, 6315 (1986).

17) M. Drabbels, J. Heinze, and W. L. Meerts, *J. Chem. Phys.*, **100**, 165 (1994).

18) P. Dupre, R. Jost, M. Lombardi, P. G. Green, E. Abramson, and R. W. Field, *Chem. Phys.*, **152**, 293 (1991).

19) N. Ochi and S. Tsuchiya, *Chem. Phys. Lett.*, **140**, 20 (1987); *Chem. Phys.*, **152**, 319 (1991).

20) H. Abe and H. Hayashi, *Chem. Phys. Lett.*, **206**, 337 (1993).

21) K. S. Shin and J. V. Michael, *J. Phys. Chem.*, **95**, 5864 (1991).

22) S. Satyapal and R. Bersohn, *J. Phys. Chem.*, **95**, 8004 (1991).

23) K. Seki and H. Okabe, *J. Phys. Chem.*, **97**, 5284 (1993).

24) H. Okabe, *J. Chem. Phys.*, **75**, 2772 (1981); **78**, 1312 (1983).

25) A. H. Laufer, *J. Chem. Phys.*, **73**, 49 (1980).

26) A. H. Laufer, *Chem. Phys. Lett.*, **94**, 240 (1983).

27) A. H. Laufer, *J. Photochem.*, **27**, 267 (1984).

28) A. Fahr and A. H. Laufer, *J. Phys. Chem.*, **89**, 2906 (1985); **90**, 5064 (1986).

29) M. N. R. Ashfold, D. H. Mordaunt, and S. H. S. Wilson, in "Advances in Photochemistry," ed by D. Neckers, D. Volman, and G. von Bunau, Vol. 21, 1995.

30) A. M. Wodtke and Y. T. Lee, *J. Phys. Chem.*, **89**, 4744 (1985).

31) H. Shiromura, Y. Achiba, K. Kimura, and Y. T. Lee, *J. Phys. Chem.*, **91**, 17 (1987).

32) Y. Chen, D. M. Jonas, C. E. Hamilton, P. G. Green, J. K. Kinsey, and R. W. Field, *Ber. Bunsenges. Phys. Chem.*, **92**, 329 (1988).

33) L. A. Curtiss and J. A. Pople, *J. Chem. Phys.*, **91**, 2420 (1989).

34) J. Segall, R. Lavi, Y. Wen, and C. Wittig, *J. Phys. Chem.*, **93**, 7287 (1989).

35) P. G. Green, J. K. Kinsey, and R. W. Field, *J. Chem. Phys.*, **91**, 5160 (1989).

36) J. A. Montgomery, Jr., and G. A. Petersson, *Chem. Phys. Lett.*, **168**, 75 (1990).

37) C. W. Bauschlicher, Jr., S. R. Langhoff, and P. R. Taylor, *Chem. Phys. Lett.*, **171**, 42 (1990).

38) C. J. Wu and E. A. Carter, *J. Am. Chem. Soc.*, **112**, 5893 (1990).

39) K. M. Ervin, S. Gronert, S. E. Barlow, M. K. Gilles, A. G. Harrison, V. M. Bierbaum, C. H. DePuy, W. C. Lineberger, and G. B. Ellison, *J. Am. Chem. Soc.*, **112**, 5750 (1990).

40) B. Ruscic and J. Berkowitz, *J. Chem. Phys.*, **93**, 5586 (1990).

41) D. P. Baldwin, M. A. Buntine, and D. W. Chandler, *J. Chem. Phys.*, **93**, 6578 (1990).

42) B. A. Balko, J. Zhang, and Y. T. Lee, *J. Chem. Phys.*, **94**, 7958 (1991).

43) D. H. Mordaunt and M. N. R. Ashfold, *J. Chem. Phys.*, **101**, 2630 (1994).

44) S. H. S. Wilson, M. N. R. Ashfold, and R. N. Dixon, *J. Chem. Phys.*, **101**, 7538 (1994), and references therein.

45) H. Kanamori and E. Hirota, *J. Chem. Phys.*, **88**, 6699 (1988).

46) G. Herzberg, "Molecular Spectra and Molecular Structure," Van Nostrand Reinhold, New York (1945), Vol. 2.

47) T. R. Huet, M. Herman, and J. W. C. Johns, *J. Chem. Phys.*, **94**, 3407 (1991).

48) M. E. Jacox, *J. Phys. Chem. Ref. Data*, **19**, 1387 (1990).

49) D. Forney, M. E. Jacox, and W. E. Thompson, *J. Mol. Spectrosc.*, **170**, 178 (1995).